MRI and tumor biochemistry: Gallagher and colleagues provide an overview of hyperpolarized ^{13}C MR spectroscopic imaging and compare sensitivity, spatial and temporal resolution, and risks with those of PET imaging. . . . . ***Page 1333***

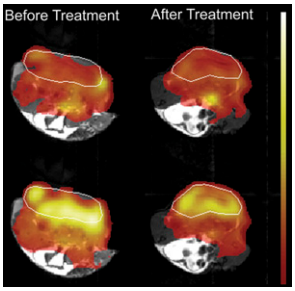

P-selectin cardiovascular imaging: Boersma and colleagues look at the potential challenges for imaging this adhesion molecule and activation marker in atherosclerotic disease and preview a related article in this issue of *JNM*. . . . . ***Page 1337***

^{18}F-fluoropaclitaxel PET/CT: Kurdziel and colleagues describe radiation dosimetry and imaging studies in healthy adults and women with breast cancer and the potential for use of intratumoral ^{18}F-fluoropaclitaxel distribution as a surrogate for paclitaxel in solid tumors. . . . . ***Page 1339***

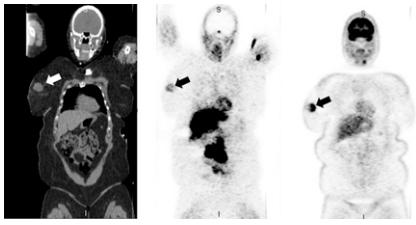

Hand-held preoperative SLN camera: Kerrou and colleagues compare the effectiveness of a hand-held preoperative compact γ-camera for sentinel lymph node detection in breast cancer with that of conventional lymphoscintigraphy. . . . . ***Page 1346***

Network assessment of lymphoma RIT: Hohloch and colleagues present the work of the Radioimmunotherapy Network, a Web-based international registry collecting long-term observational data about radioimmunotherapy-treated patients with malignant lymphoma outside randomized clinical studies. . . . . ***Page 1354***

Quality of life after ^{177}Lu-octreotate: Khan and colleagues investigate quality of life and symptoms after therapy with this peptide-receptor radionuclide therapy in patients with inoperable or metastasized gastroenteropancreatic or bronchial neuroendocrine tumors. . . . . ***Page 1361***

Coronary function and metabolic syndrome: Di Carli and colleagues explore the hypothesis that metabolic syndrome is associated with impaired coronary vasodilator function, a marker of atherosclerotic disease activity. . . . . ***Page 1369***

^{123}I-MIBG uptake in pulmonary emphysema: Suga and colleagues evaluate impaired lung uptake of ^{123}I-MIBG on SPECT in patients with pulmonary emphysema and compare the results with those from perfusion SPECT and morphologic CT. . . . . ***Page 1378***

PET and cervical myelopathy: Floeth and colleagues investigate the role of ^{18}F-FDG PET in patients with degenerative stenosis of the cervical spinal cord and look at correlations with postsurgical outcomes. . . . . ***Page 1385***

MRI-based AC for PET/MR: Hofmann and colleagues assess 2 algorithms for whole-body MRI-based PET attenuation correction and describe potential benefits for routine clinical hybrid PET/MRI. . . . . ***Page 1392***

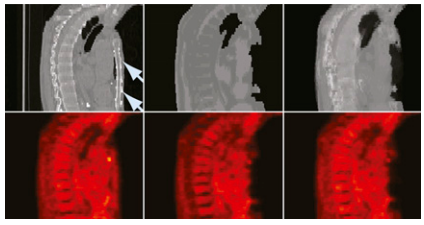

SPECT and carotid endarterectomy: Sato and colleagues research the ability of preoperative central benzodiazepine receptor binding potential and cerebral blood flow imaging with SPECT to identify patients at risk for new cerebral ischemic events after carotid endarterectomy. . . . . ***Page 1400***

Thrombus in aneurysm on PET/CT: Muzaffar and colleagues evaluate the incidence of aneurysm and the frequency of thrombus within an aneurysm on unenhanced ^{18}F-FDG PET/CT studies. . . . . ***Page 1408***

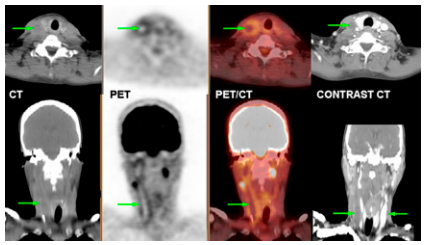

Somatostatin receptor antagonist imaging: Wild and colleagues describe somatostatin receptor antagonist imaging studies in patients with metastatic thyroid carcinoma or neuroendocrine tumors and discuss the advantages such imaging would provide in peptide receptor–mediated imaging and therapy. . . . . ***Page 1412***

^{131}I-MIBG extravasation: Bonta and colleagues report on a new catheter placement protocol for therapeutic administration of ^{131}I-MIBG and detail the extravasation incident that prompted institution of this protocol. . . . . ***Page 1418***

Fukushima accident response perspectives: Dauer and colleagues offer an educational review of the short-term chronology, radiologic consequences, emergency responses, and long-term challenges associated with the March 2011 nuclear power facility events in Japan. . . . . ***Page 1423***

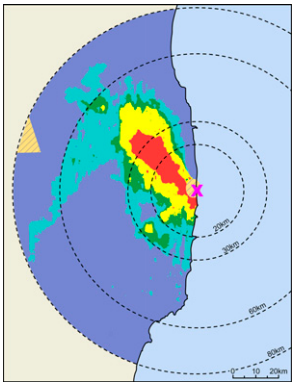

P-selectin imaging with ^{99m}Tc-fucoidan: Rouzet and colleagues propose a new approach to molecular imaging of overexpression of platelet and endothelial P-selectin. . . . . ***Page 1433***

^{18}F-octreotate PET: Leyton and colleagues compare in vitro affinity and tissue pharmacokinetics of 5 structurally related ^{19}F/^{18}F-fluoroethyltriazole-Tyr^3-octreotate analogs and discuss the potential for more rapid clinical protocols for gastroenteropancreatic neuroendocrine tumor imaging with PET. . . . . ***Page 1441***

α_7nAChR PET tracer: Ettrup and colleagues offer details on ^{11}C-NS14492, a selective α_7 nicotinic acetylcholine receptor agonist PET radioligand that may prove useful in evaluation and selection of appropriate drug candidates in schizophrenia and Alzheimer disease. . . . . ***Page 1449***

Quantum dot EGFR imaging: Jung and colleagues explore the potential of a novel quantum dot–based technique targeting the epidermal growth factor receptor, with promise for quantitatively monitoring receptor status and treatment response in breast cancer. . . . . ***Page 1457***

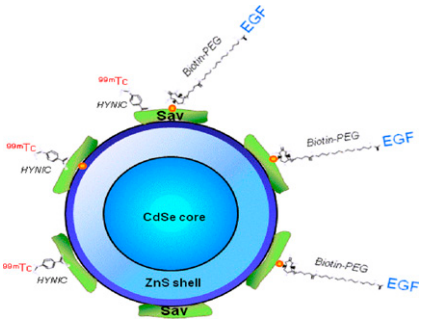

RIT agent for AML: Leyton and colleagues characterize ^{111}In-nuclear translocation sequence-7G3, an Auger electron–emitting radioimmunotherapeutic agent with potentially beneficial applications in acute myelogenous leukemia. . . . . ***Page 1465***

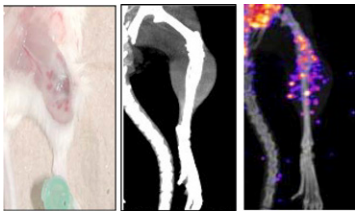

Dosimetry of ^{99m}Tc-HYNIC-TOC: Grimes and colleagues report on the biodistribution and radiation dosimetry of this somatostatin receptor–targeting agent in patients with suspected neuroendocrine tumors undergoing whole-body dynamic planar and SPECT/CT imaging. . . . . ***Page 1474***

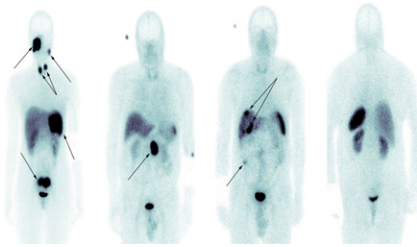

MRI assessment of marrow cellularity: Pichardo and colleagues extend the IDEAL technique for estimating fat fractions to the derivation of data for estimation of patient-specific bone marrow mass using published predictive equations. . . . . ***Page 1482***

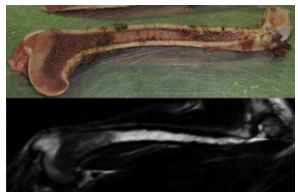

First-in-human study of BMS747158: Maddahi and colleagues evaluate radiation dosimetry, biodistribution, safety, tolerability, and early elimination in urine of a single injected dose of this ^{18}F-labeled myocardial perfusion imaging tracer that targets mitochondrial complex 1. . . . . ***Page 1490***

ON THE COVER

^{99m}Tc-fucoidan has been found to be a relevant imaging agent for in vivo detection of biologic activities associated with P-selectin overexpression, such as arterial thrombus and ischemic memory, and overcomes some limitations of previous P-selectin–targeted agents. In the above SPECT/CT slices of a rat with aortic valve endocarditis, ^{99m}Tc-fucoidan uptake is seen in the aortic valve area.

See page 1436.